CHAPTER VI
EFFECT OF CO-DOPANTS ON HYDROGEN DESORPTION/ABSORPTION OF METAL-DOPED $NaAlH_4$

6.1 Abstract

The segregation of bulk Al after the hydrogen desorption may be one of many reasons why there is the incomplete hydrogen re-absorption and the need for higher desorption temperature in the subsequent desorption of metal-doped $NaAlH_4$. In this work, we attempted to improve the reversible hydrogen storage capacity of 4 mol% $HfCl_4$ doped $NaAlH_4$ by adding 10 wt% co-dopant (activated carbon, graphite, and carbon nanotubes) using ball milling technique. It was found that the co-dopants significantly affect the hydrogen desorption/re-absorption of the hydride. The hydrogen re-absorption capacity of $HfCl_4$ doped $NaAlH_4$ added with the co-dopants increases 10-30% as compared with that without a co-dopant, and graphite seems to be the best co-dopant among three tested carbon materials. Furthermore, graphite also shows the good synergy with other metal catalysts ($TiCl_3$, TiO_2, Ti, and VCl_3) on the reversibility enhancement of $NaAlH_4$. $TiCl_3$-$NaAlH_4$ added with graphite has the highest hydrogen capacity around 4 wt% (H/M). Moreover, the rate of hydrogen re-absorption of co-dopant doped samples also increases more than 50% of that without a co-dopant. Thus, it can be postulated that high porosity and large surface area of the co-dopant decrease the segregation of bulk Al after the desoprtion and improve hydrogen diffusion in or out from the bulk of desorbed or re-absorbed samples.

6.2 Introduction

$NaAlH_4$ (Sodium aluminium hydride) has been considered to be a promising solid media for hydrogen storage especially after the discovery by Bogdanović and Schwickardi on the reversibility of $NaAlH_4$ by doping with small amounts of metal catalysts [1-2]. The modified $NaAlH_4$ with metal catalysts can desorb/re-absorb hydrogen at a moderate condition. Metal catalysts in the Group 4 (Ti, Zr, and, Hf)

seem to be effective dopants in the reaction. $TiCl_3$ by far shows the best catalytic activity in the hydrogen desorption/absorption. However, the cycling hydrogen storage capacity of $NaAlH_4$ doped with metal catalysts is around 1.5 - 4 wt%, which is lower than the theoretical hydrogen capacity, 5.6 wt% [3-14].

In our previous work, we studied the hydrogen desorption/absorption of $NaAlH_4$ doped with Ti-, Zr-, Hf-, or V-compound. The reversible hydrogen capacity is around 1.5-3.8 wt% (H/M) based on the only metal hydride weight [12]. One reason that the total reversibility of the desorbed sample cannot be achieved to the original state may be because of the segregation of bulk Al after the hydrogen desorption. This, in turn, decreases the surface area for hydrogen diffusion. If, somehow, the segregation of Al could be prevented, which would result in a better hydrogen transfer in the Al bulk, the hydrogen re-absorption in the sample may possibly be increased. To achieve that aim, co-doping a porous material with a transition metal catalyst in $NaAlH_4$ may be of help for the quest to obtain high hydrogen reversibility. In fact, attempts have been made by doping carbon nanostructures with transition metal catalysts in $NaAlH_4$ to improve their hydrogen desorption/re-absorption [15-18].

The main objective of this work is to investigate the effect of graphite, activated carbon, and carbon nanotubes on the hydrogen desorption/absorption of metal doped $NaAlH_4$.

6.3 Experimental

6.3.1 Materials

$NaAlH_4$ (90% purity), $HfCl_4$ (98% purity), Ti powder (99.98%, 325 mesh), and graphite (99.99%) were purchased from Aldrich Chemical. VCl_3 (99% purity) was purchased from Merck. TiO_2 (P25) was ordered from Degüssa. Activated carbon was obtained from CALGON, BPL. $TiCl_3$ (Riedel-de Haën) was obtained from vacuum drying of 12% $TiCl_3$ in hydrochloric acid (see detail of the preparation in Chapter 3).

While carbon nanotubes (CNTs) - multi walled type - was synthesized and treated with the following method. Prior to experiments, $LaNi_5$

(Guangzhou Research Institute for Non-Ferrous Metals, China) used as a catalyst was treated by stirring with 0.2 M HCl for 30 min then filtered and washed with deionized water. About 2 g of treated $LaNi_5$ was loaded into a quartz combustion boat and placed inside a quartz tube located inside a tube furnace. The system was sealed and flushed with nitrogen for 10 min, and then the temperature was ramped to 800°C. Once the temperature was stabilized, the nitrogen flow was cut off and liquid petroleum gas (LPG, Afrox South Africa) flow was initiated at a flow rate of 5.8 cm^3 min^{-1}. After 60 min, the LPG flow was terminated and the nitrogen flow was re-initiated. The sample was then cooled under nitrogen. To purify CNTs obtained from the synthesis, 2 g of CNTs were added to 100 ml of 10 M HCl. The mixture was sonicated (ultrasonic bath, integral systems, model UMC-20, 50 kHz, 400 watts) for 1 h and refluxed at 120°C for 3 h. The solid was filtered and washed with deionized water until pH value of the rinsed water was around 6-7, and dried in an oven at 90°C overnight. Before metal deposition, the purified CNTs were modified through oxidation by concentrated HNO_3 under ultrasonication for 1 h.

6.3.2 Hydrogen desorption/absorption

All experiments in this study were performed under nitrogen atmosphere from a cryogenic source. $NaAlH_4$ was doped with 4 mol% $HfCl_4$ together with one of co-dopants including graphite, activated carbon, and CNTs. An amount of co-dopant is 10 wt%. A centrifugal ball mill (Retsch ball mill model S100, stainless steel vial size 250 ml, stainless balls with 1 cm and 2 cm diameters) was used as a mixing means for 20 min with a speed of 300 rpm.

After the mixing, approximately 1 g of a sample was placed into a thermovolumetric apparatus. The high pressure stainless steel reactor (316SS) was heated from room temperature to 280°C via a furnace controlled by a PID temperature controller. The K-type thermocouple was placed inside the reactor to measure the temperature. The pressure transducer (Cole Parmer, model 68073-68074) was used to keep track of the pressure change resulted from hydrogen desorption. For absorption experiments, hydrogen (99.9995%) was used to pressurize the high pressure vessel. Hydrogen was re-absorbed at 120°C and 10 MPa for 10 h. Once the pressure reading was constant over a period of time, the data was used to

calculate the amount of hydrogen absorbed on the sample. The released hydrogen shown in wt% (H/M) was calculated with respect to only the amount of $NaAlH_4$ while wt% was calculated with respect to the amount of $NaAlH_4$ plus a metal and co-dopant in the sample. The same procedure was repeated to investigate the reversibility.

Sample characterization was performed using a Rigaku X-ray diffractometer at room temperature over a range of diffraction angles from 28-70 with CuK-alpha radiation (40 kV, 30 mA).

6.4 Experimental Results

Figure 6.1 displays the 1st hydrogen desorption of $NaAlH_4$ doped with 4 mol% $HfCl_4$ ($HfCl_4$, Figure 6.1(a)) compared with the one doped with 4 mol% $HfCl_4$ and 10 mol% co-dopant: 4 mol% $HfCl_4$ + 10 wt% graphite ($HfCl_4$+G, Figure 6.1(b)), 4 mol% $HfCl_4$ + 10 wt% activated carbon ($HfCl_4$+ AC, Figure 6.1(c)), and 4 mol% $HfCl_4$ + 10 wt% CNTs ($HfCl_4$+CNTs, Figure 6.1(d)). The figure shows that the samples co-doped with 10 wt% carbon materials release hydrogen at a lower temperature (~20 - 40°C lower) than the sample only doped with $HfCl_4$ (120°C) at the initial hydrogen desorption. However, trends of their hydrogen desorption behavior are quite similar. That is the hydride samples decomposes in 2 steps with the highest released hydrogen about 4.8 wt% (H/M).

After the first hydrogen desorption, hydrogen was re-absorbed into the samples at 120°C with an initial pressure of 10 MPa for 10 h. Figure 6.2 shows that the hydrogen re-absorption rates of samples doped with $HfCl_4$ and the carbon materials are 50% higher than that of the one doped only with $HfCl_4$. The initial rate of hydrogen re-absorption were also calculated: 0.012 wt% (H/M) min^{-1} for $HfCl_4$, 0.035 wt% (H/M) min^{-1} for $HfCl_4$+G, 0.019 wt% (H/M) min^{-1} for $HfCl_4$+AC, and 0.032 wt% (H/M) min^{-1} for $HfCl_4$+CNTs. The sample co-doped with graphite shows the best performance in hydrogen re-absorption using about 4 h to reach the maximum hydrogen re-absorption while the ones doped with activated carbon or CNTs needs 5 and 6 h, respectively.

Figure 6.3 shows the hydrogen reversibility in the samples doped with 4 mol% $HfCl_4$ and 10 wt% co-dopant compared with the one doped with only 4 mol% $HfCl_4$. The results reveal that all co-dopants increase the amount of the re-absorbed hydrogen and decrease the desorption temperature in subsequent cycles compared to $NaAlH_4$ doped with only $HfCl_4$. An increase about 10-30% of the re-absorbed hydrogen amount from the sample without any co-dopant can be observed. The sample with $HfCl_4$ and graphite re-absorbs hydrogen up to 3.5 wt% (H/M) and the re-absorbed amounts are lower with CNTs (3.2 wt% (H/M)) and activated carbon (3 wt% (H/M)) while the reversible hydrogen capacity of the sample without a co-dopnat is around 2.6 wt% (H/M). Moreover, the initial hydrogen desorption in the subsequent cycle of the samples added with activated carbon occurs at the lower temperature, 135°C while the one without a co-dopant is at 150°C. Comparison between the reversibility of $NaAlH_4$ co-doped with the carbon materials indicates that the stability of the reversible hydrogen capacity of the sample co-doped with activated carbon is inferior to the other samples, which are co-doped with graphite or carbon nanotubes. The reversible capacity of $HfCl_4$-$NaAlH_4$ co-doped with activated carbon tends to decrease with the increase in the number of cycles.

A possible reason for the improvement of the hydrogen desorption/re-absorption of $NaAlH_4$ with the co-dopants could be the role of their physical properties (porosity and high surface area) as it is these properties that may help in increasing the hydrogen transfer in and out from the bulk sample by decreasing the grain aggregation of desorbed $NaAlH_4$ as reported by Cento *et al.* [19]. Moreover, as carbon materials are known to posses unique properties as a mixing agent manifested through lubrication phenomena and as micro-grinding agent manifested through the formation of carbide species, the co-dopants could facilitate the mixing during the sample preparation and increase the hydrogen diffusion hydrogen pathway into the desorbed hydride sample.

In addition, the role of carbon materials may involve with the electronic effect to promote the activity of metal catalysts in the hydrogen desorption/re-absorption of $NaAlH_4$. The π-electron of carbon is known to be back-donated to the lower energy partially empty d-orbitals of metal catalyst leading to enhance the activity of catalyst in the reaction [18]. Moreover, the hydrogen spillover mechanism

also facilitates the hydrogen diffusion hydrogen pathway into the desorbed hydride sample.

Among the studied co-dopants, graphite exhibits the best activity with the transition metal catalysts on the hydrogen desorption/re-absorption of $NaAlH_4$. The different performance of each carbon material on the reaction may be explained in terms of carbon structure. The planar carbon structures (graphite) tend to favor easier hydrogen penetration during the hydrogen re-absorption than tridimensional ones (activated carbon or CNTs) [20]. Moreover, the carbonyl group on the carbon surface of activated carbon and CNTs may partially retard or block hydrogen diffusion into the hydride system if an oxide film on the surface is formed. This may cause the lower reversibility of the sample doped with $HfCl_4$ and activated carbon in the prolonged cycles.

The XRD patterns of $HfCl_4$-$NaAlH_4$, $HfCl_4$+G-$NaAlH_4$, $HfCl_4$+AC-$NaAlH_4$, and $HfCl_4$+CNTs-$NaAlH_4$ after desorption and re-absorption in Figures 6.4 and 6.5 show that products after complete decomposition consist of NaH, Al and NaCl, while the constituents are $NaAlH_4$, Na_3AlH_6, Al, and NaCl for the re-absorbed hydride. No peak of other compounds is present from the characterization. This may indicate that no new crystal phase was formed after co-doping the carbon materials in the hydride system [15-18].

To further confirm the role of graphite in improving the reversibility of metal-doped $NaAlH_4$, 10 wt% graphite was also co-doped in VCl_3-, metallic Ti-, TiO_2-, and $TiCl_3$-doped $NaAlH_4$. Figures 6.6 - 6.9 display the comparison between hydrogen desorption in the 1st desorption and 7th desorption of the samples co-doped with graphite and the ones without graphite. It was found that co-doping graphite can increase the reversible hydrogen capacity of $NaAlH_4$ with metal and graphite, 5-70% higher than the ones without graphite. Moreover, graphite dramatically influences the 1st cycle of hydrogen desorption of VCl_3-$NaAlH_4$ co-doped with graphite and Ti-$NaAlH_4$ co-doped with graphite by decreasing the desorption temperature of the hydride samples. Figure 6.6 reveals that the desorption temperature of VCl_3-$NaAlH_4$ co-doped with graphite is about 20-40°C lower than the sample without graphite. The decrease in the desorption temperature is also observed in the subsequent cycle. The reversible hydrogen capacity of VCl_3-$NaAlH_4$ is increased from 1.5 wt% (H/M)

to 2.7 wt% (H/M) after adding graphite. Figure 6.7 displays the effect of graphite on the hydrogen desorption of Ti-$NaAlH_4$. Although adding graphite in Ti-$NaAlH_4$ clearly decreases the 1st desorption temperature (~ 40°C lower), a small amount of reversible hydrogen capacity can be increased from 0.97 wt% (H/M) for Ti-$NaAlH_4$ to 1.38 wt% (H/M) for the one added with graphite. This can be infered that the activity of metal catalyst in hydrogen dissociation has more influence on the reversible hydrogen capacity of $NaAlH_4$. In the case of TiO_2-$NaAlH_4$ and $TiCl_3$ added with graphite (Figures 6.8 and 6.9), their hydrogen desorption behaviors are not changed after the samples added with graphite. Less than 5% of the reversible hydrogen capacity of TiO_2-$NaAlH_4$ and $TiCl_3$-$NaAlH_4$ is increased after adding graphite, 3.95 wt% (H/M) to 3.99 wt% (H/M).

Although doping carbon materials can improve the hydrogen re-absorption and increase hydrogen capacity in the hydride system, they also increase the total weight of the sample. As the amount of released hydrogen of the samples were calculated with respect to total weight of sample (wt%), it was noticed that the reversible hydrogen capacity of all metal doped $NaAlH_4$ increases after co-doping with graphite, except TiO_2- and $TiCl_3$-$NaAlH_4$ co-doped with graphite, which are lower than that of the sample without graphite as shown in Figure 6.10.

6.5 Conclusions

Adding carbon materials (graphite, activated carbon, and CNTs) significantly improve the hydrogen re-absorption rate and increase the reversible hydrogen capacity of metal doped $NaAlH_4$. The hydrogen re-absorption capacity of metal-doped $NaAlH_4$ added with the co-dopants increases 5-70% from that without a co-dopant, and graphite seems to be the best co-dopant. Moreover, the co-dopants catalyze the hydrogen desorption of $NaAlH_4$ by lowering 20-40°C of the desorption temperature. It may be explained that the high porosity and large surface area of the co-dopant would decrease the segregation of Al bulk after the desorption and improve the hydrogen diffusion in/out from the bulk of desorbed/re-absorbed samples. Moreover, carbon materials might involve with the electronic effect to

promote the activity of metal catalysts in the hydrogen dissociation into the desorbed hydride.

6.6 Acknowledgements

This work was supported by the National Science and Technology Development Agency (Reverse Brain Drain Project); the Petroleum and Petrochemical College (PPC), the Research Unit for Petrochemical and Environment Catalysts, the Ratchadapisek Somphot Endowment, and National Center of Excellence for Petroleum, Petrochemicals and Advanced Materials, Chulalongkorn University; and UOP LLC.

6.7 References

[1] Fakioğlu E, Yűrűm Y, Veziroğlu TN. A review of hydrogen storage based on boron and its compounds. Int. J. Hydrogen Energy 2004;29:1371-1376.

[2] Bogdanović B, Schwickardi M. Ti-doped alkali metal aluminium hydrides as potential novel reversible hydrogen storage materials. J. Alloys Compd 1997;253-254:1-9.

[3] Zidan A, Takara S, Hee A, Jensen CM. Hydrogen cycling behavior of zirconium and titanium-zirconium-doped sodium aluminum hydride. J. Alloys Compd 1999;285:119-122.

[4] Jensen M, Zidan R, Mariels N, Hee A, Hagen C. Advance titanium doping of sodium aluminum hydride: segue to a pratical hydrogen storage material? Int. J. Hydrogen Energy 1999;24:461-465.

[5] Bogdanović B, Brand RA, Marjanovic A, Schwickardi M, Tolle J. Metal-doped sodium aluminium hydrides as potential new hydrogen storage materials. J. Alloys Compd 2000;302:36-58.

[6] Sandrock G, Gross K, Thomas G. Effect of Ti-catalyst content on the reversible hydrogen storage properties of the sodium alanates. J. Alloys Compd 2002;399:299-308.

[7] Gross KJ, Majzoub EH, Spangler SW. The effects of titanium precursors on hydriding properties of alanates. J. Alloys Compd 2003;356-357:423-428.

[8] Anton DL. Hydrogen desorption kinetics in transition metal modified $NaAlH_4$. J. Alloys Compd 2003;356-357:400-404.

[9] Weidenthaler C, Pommerin A, Felderhoff M, Bogdanović B, Schüth F. On the state of the titanium and zirconium in Ti- or Zr-doped $NaAlH_4$ hydrogen storage material. Phys. Chem. Chem. Phys. 2003;5:5149-5153.

[10] Schüth F, Bogdanović B, Felderhoff M. Light metal hydrides and complex hydrides for hydrogen storage. Chem. Commun. 2004:2249-2258.

[11] Suttisawat Y, Jannatisin V, Rangsunvigit P, Kitiyanan B, Muangsin N, Kulprathipanja S. Catalytic effect of Zr and Hf on hydrogen desorption/absorption of $NaAlH_4$ and $LiAlH_4$. Int. J. Hydrogen Energy 2007;32:1277-1285.

[12] Suttisawat Y, Jannatisin V, Rangsunvigit P, Kitiyanan B, Muangsin N, Kulprathipanja S. Understanding the effect of TiO_2, VCl_3, and $HfCl_4$ on hydrogen desorption/absorption of $NaAlH_4$. J. Power Sources 2007;163:997-1002.

[13] Xiao X, Chen L, Wang X, Wang Q, Chen C. The hydrogen storage properties and microstructure of Ti-doped sodium aluminum hydride prepared by ball-milling. Int. J. Hydrogen Energy 2007;32:2475-2479.

[14] Orimo S, Nakamori Y, Eliseo JR, Züttet A, Jensen CM. Complex hydrides for hydrogen storage. Chem. Rev. 2007;107:4111-4132.

[15] Wang J, Ebner AD, Ritter JA. Kinetic behavior of Ti-doped $NaAlH_4$ when cocatalyzed with carbon nanostructures. J. Phys. Chem. B 2006;110:17353-17358.

[16] Wang J, Ebner AD, Prozorov T, Zidan R, Ritter JA. Synergistic effects of co-dopants on the dehydrogenation kinetics of sodium aluminum hydride. J. Alloys Compd 2005;391:245-255.

[17] Wang J, Ebner AD, Prozorov, T, Zidan R, Ritter, JA. Effect of graphite as a co-dopant on the dehydrogenation and hydrogenation kinitics of Ti-doped sodium aluminum hydride, J. Alloys Compd 2005;395:252-262.

[18] Dehouuche Z, Lafi L, Grimard N, Goyette J, Chahine R. The catalytic effect of single-wall carbon nanotubes on the hydrogen sorption properties of sodium alanates. Nanotechnology 2005;16:402-409.

[19] Cento C, Gislon P, Bilgili M, Masci A, Zheng Q, Prosini PP. How carbon affects hydrogen desorption in $NaAlH_4$ and Ti-doped $NaAlH_4$. J. Alloys Compd 2007;437:360-366.

[20] Bouaricha S, Dodelet J-P,Guay D, Huot J, Schulz R. Study of the activation process of Mg-based hydrogen storage materials modified by graphite and other carbonaceous compounds. J. Mater. Res. 2001;16:2893-2905.

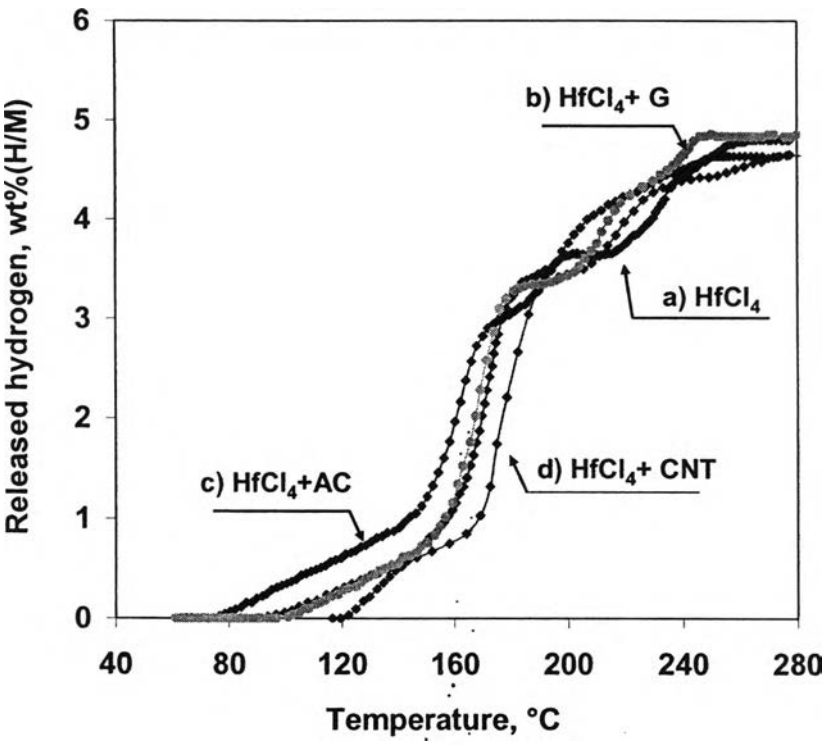

Figure 6.1 Correlation between temperature and hydrogen released during the 1st hydrogen desorption of doped $NaAlH_4$: a) 4 mol% $HfCl_4$, b) 4 mol% $HfCl_4$ + 10 wt% graphite, c) 4 mol% $HfCl_4$ + 10 wt% activated carbon, and d) 4 mol% $HfCl_4$ + 10 wt% CNTs.

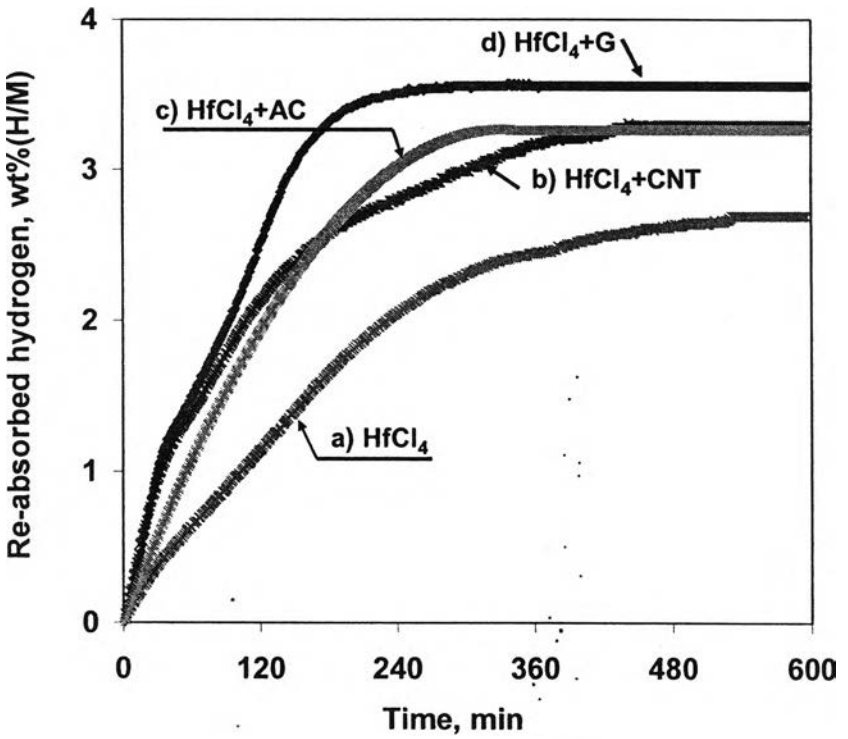

Figure 6.2 The hydrogen re-absorption rate in the 3rd cycle of doped $NaAlH_4$: a) 4 mol% $HfCl_4$, b) 4 mol% $HfCl_4$ + 10 wt% CNTs, c) 4 mol% $HfCl_4$ + 10 wt% activated carbon, and d) 4 mol% $HfCl_4$ + 10 wt% graphite.

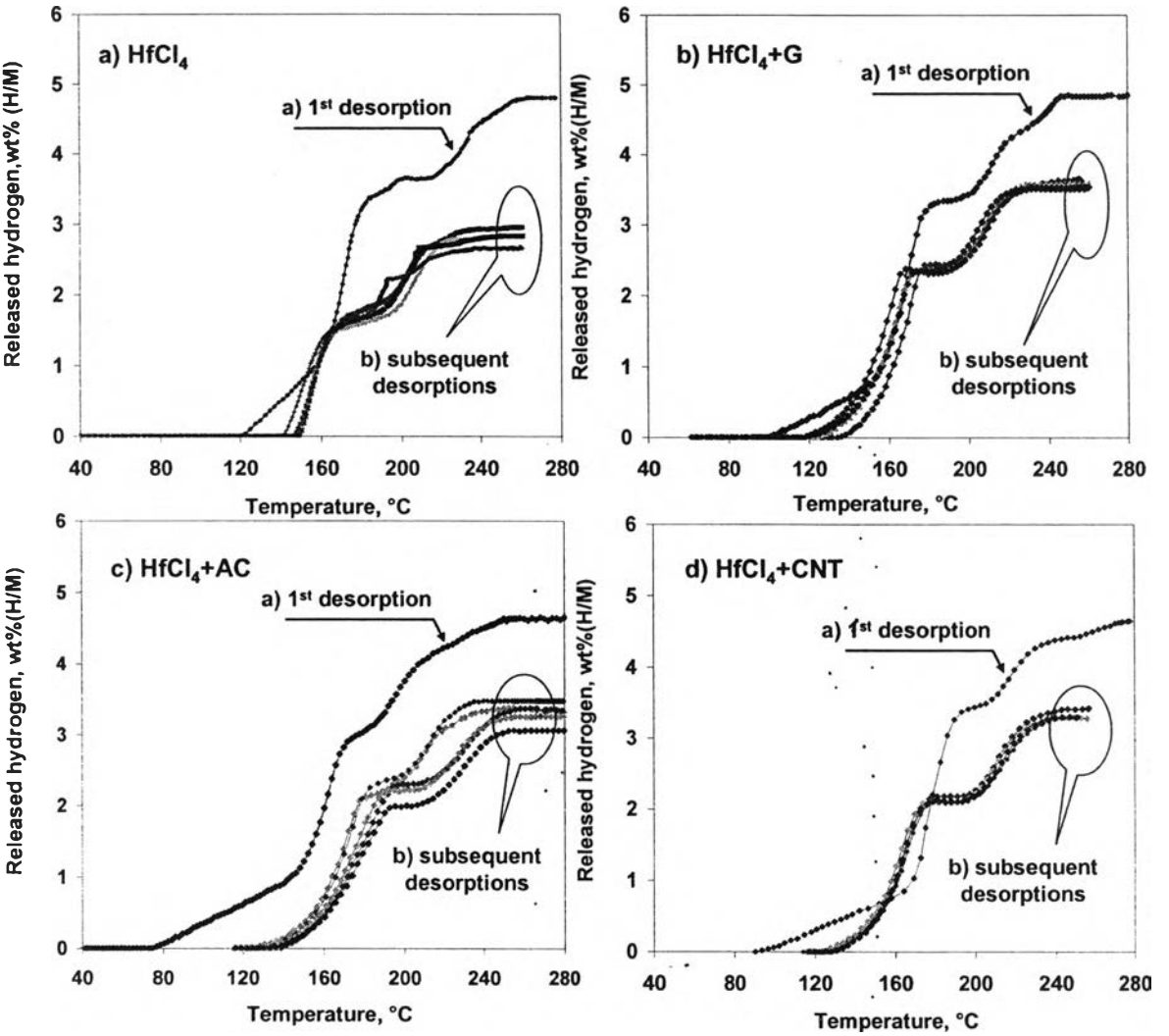

Figure 6.3 Correlation between temperature and hydrogen released compared between the 1st desorption and the subsequent desorptions of doped $NaAlH_4$: a) 4 mol% $HfCl_4$, b) 4 mol% $HfCl_4$ + 10 wt% graphite, c) 4 mol% $HfCl_4$ + 10 wt% activated carbon, and d) 4 mol% $HfCl_4$ + 10 wt% CNTs.

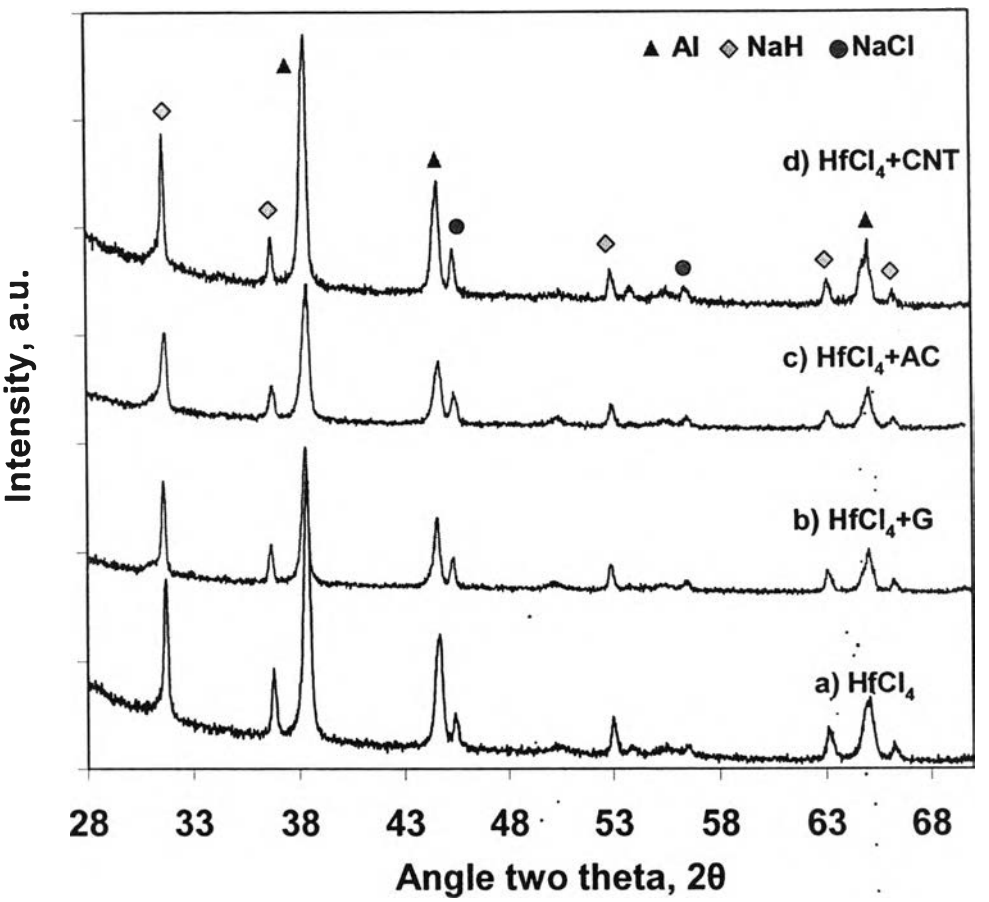

Figure 6.4 XRD patterns of a) $HfCl_4$-$NaAlH_4$, b) $HfCl_4$ + G-$NaAlH_4$, c) $HfCl_4$ + AC-$NaAlH_4$, and d) $HfCl_4$ + CNTs-$NaAlH_4$ after the hydrogen desorption.

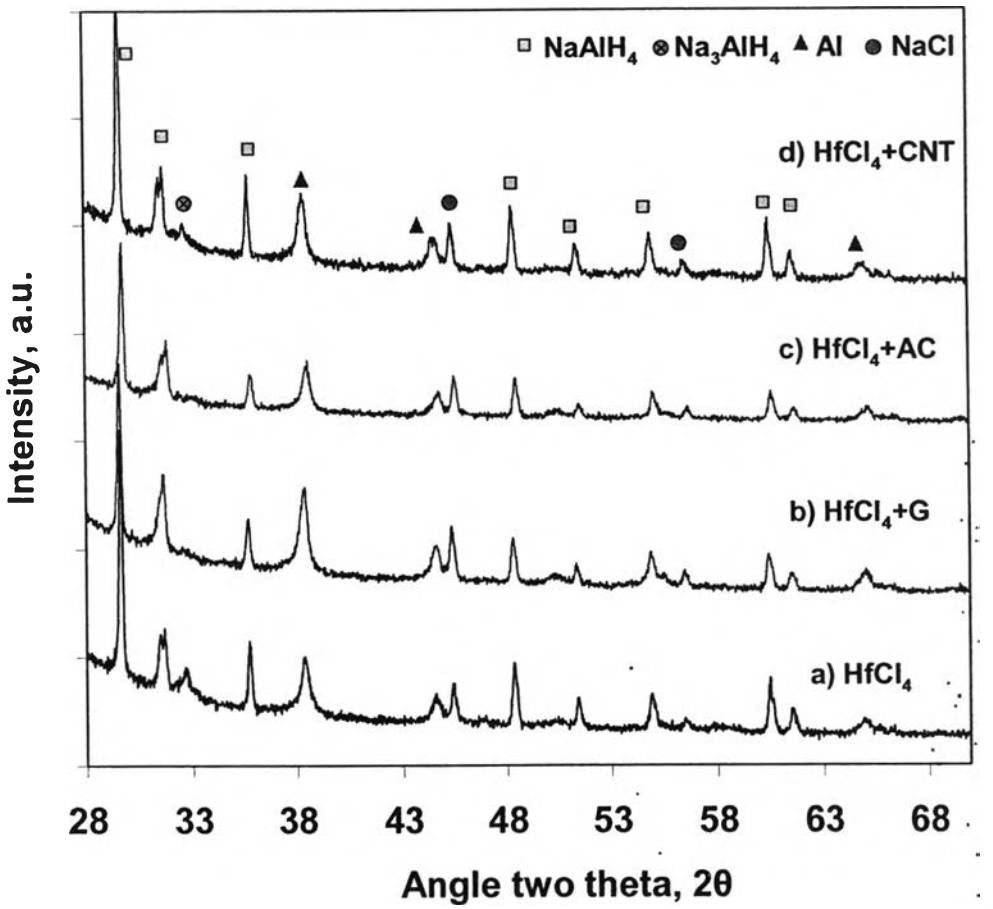

Figure 6.5 XRD patterns of a) 4 mol% $HfCl_4$-$NaAlH_4$, b) $HfCl_4$ + G-$NaAlH_4$, c) $HfCl_4$ + AC-$NaAlH_4$, and d) $HfCl_4$ + CNTs-$NaAlH_4$ after hydrogen re-absorption.

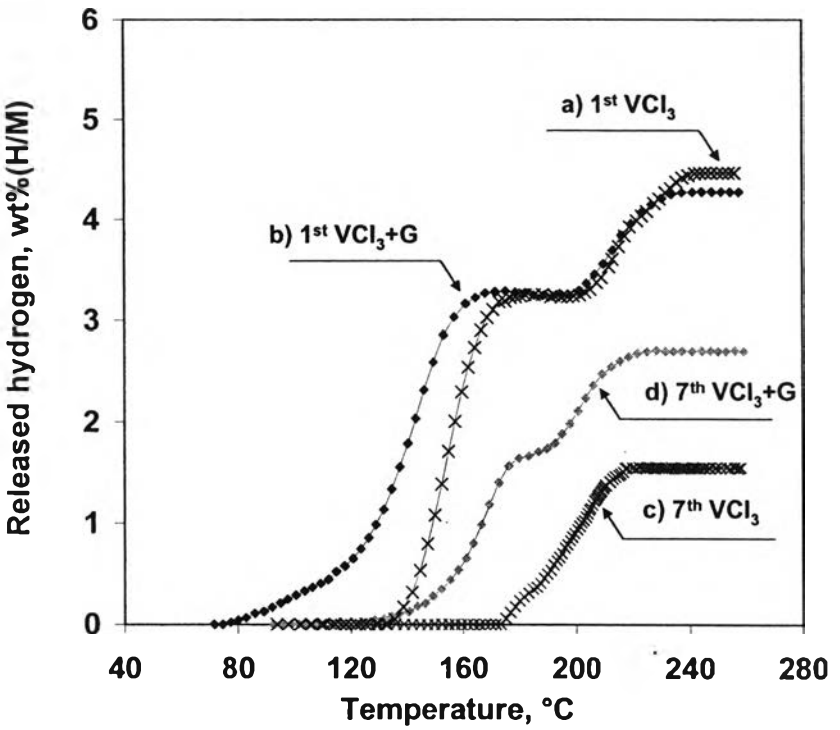

Figure 6.6 Correlation between temperature and hydrogen released during the 1st desorption of doped $NaAlH_4$ between: a) 4 mol% VCl_3 and b) 4 mol% VCl_3 + 10 wt% graphite, and in the 7th desorption: c) 4 mol% VCl_3 and d) 4 mol% VCl_3 + 10 wt% graphite.

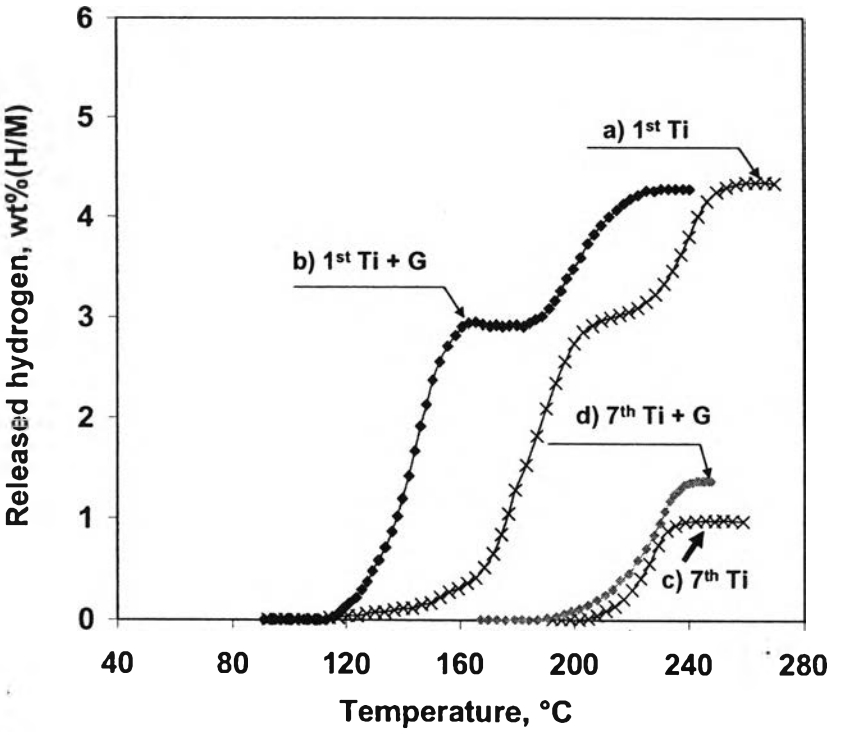

Figure 6.7 Correlation between temperature and hydrogen released during the 1st desorption of doped $NaAlH_4$ between: a) 4 mol% Ti and b) 4 mol%. Ti + 10 wt% graphite, and in the 7th desorption: c) 4 mol% Ti and d) 4 mol% Ti + 10 wt% graphite.

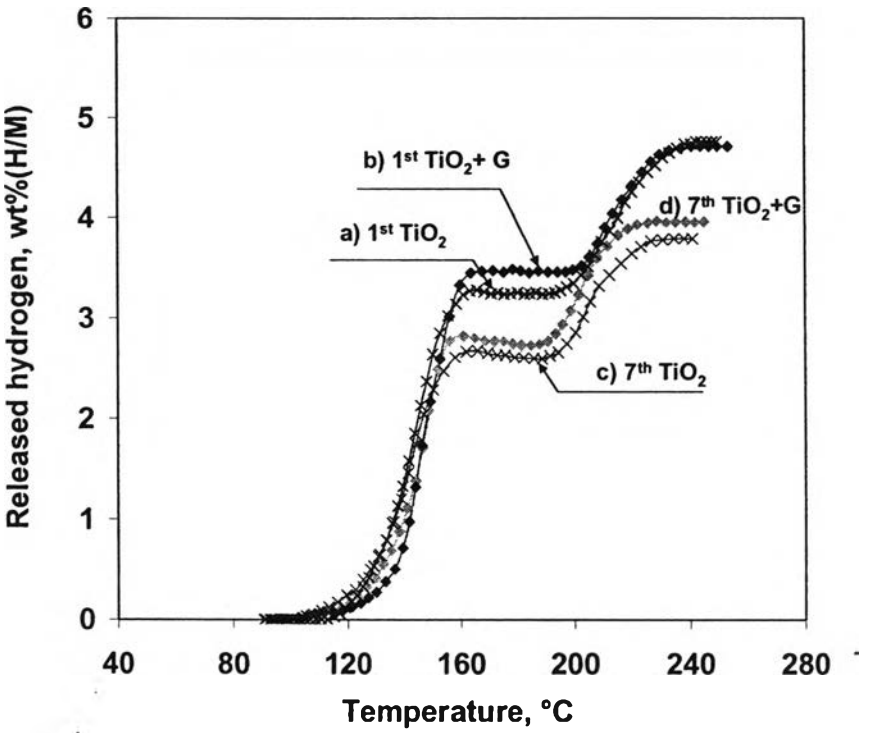

Figure 6.8 Correlation between temperature and hydrogen released during the 1st desorption of doped $NaAlH_4$ between: a) 4 mol% TiO_2 and b) 4 mol% TiO_2 + 10 wt% graphite, and in the 7th desorption: c) 4 mol% TiO_2 and d) 4 mol% TiO_2 + 10 wt% graphite.

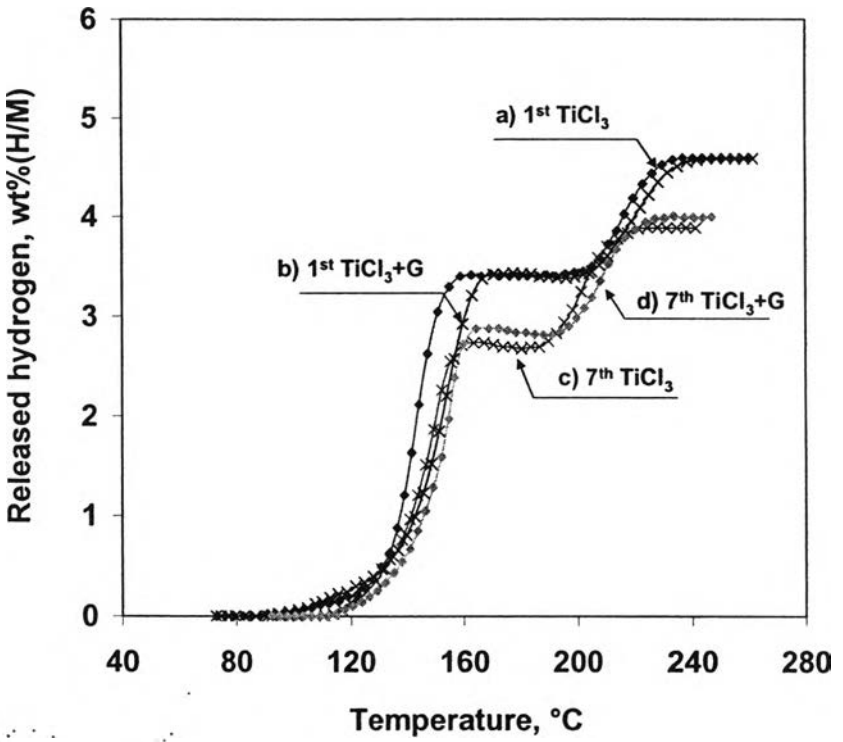

Figure 6.9 Correlation between temperature and hydrogen released during the 1st desorption of doped $NaAlH_4$ between: a) 4 mol% $TiCl_3$ and b) 4 mol% $TiCl_3$ + 10 wt% graphite, and in the 7th desorption: c) 4 mol% $TiCl_3$ and d) 4 mol% $TiCl_3$ + 10 wt% graphite.

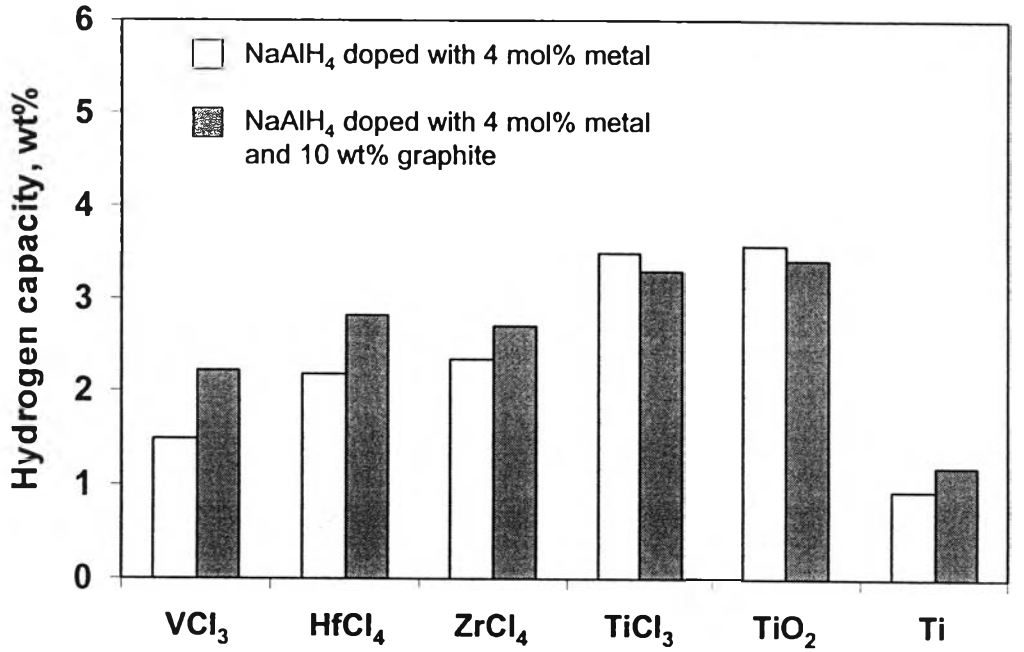

Figure 6.10 Hydrogen capacity calculated on the basis of the total weight of 4 mol% metal-$NaAlH_4$ (light block) and 4 mol% metal-$NaAlH_4$ co-doped with graphite (dark block).